MULTI-POLARIZATION SCATTEROMETER MEASUREMENTS OF LONG SURFACE GRAVITY WAVE BREAKING

Martin Gade, Thomas Alexander Grobelny, Detlef Stammer

Institut für Meereskunde, Center für Erdsytemforschung und Nachhaltigkeit (CEN), Universität Hamburg, Germany

ABSTRACT

The possibility of detecting breaking long surface gravity waves in S-band radar backscatter measurements is being investigated using multi-polarization scatterometer measurements. To detect breaking waves the change in the spectral shape of the radar Doppler spectra was analyzed with respect to possible indicators for wave breaking events. They are identified here using the ratio of the second and fourth spectral moments after normalization by the squared radar frequency. A comparison with simultaneous estimates of the fractional area of whitecaps suggests that a normalized spectral moment ratio might be used as one indicator for events of breaking surface gravity waves.

***Index Terms*—** scatterometer, wave breaking, radar backscatter, Doppler shift, whitecaps

1. INTRODUCTION

The modulation of the radar backscatter from the ocean surface by long surface gravity waves (swell) is a well-known phenomenon and has been subject to research for many years [1][4][6]. In this context, the impact of both microbreaking and long-wave (spilling) breaking on the radar return from the sea surface has been investigated [1][5][9]. Based on this earlier work, we test here the possibility whether long breaking surface gravity waves can be detected in radar backscatter measurements obtained in the Baltic. More details about the approach can also be found in [3].

2. DATA SET AND METHODOLOGY

Measurements of the radar backscatter from the sea surface are analyzed here which were performed between September 2011 and November 2013, using a multi-frequency scatterometer installed on the FINO-2 platform in the western Baltic Sea at a height of 25 meters above sea level. Details about the instruments, the measurements and the campaign are provided by [10]. The instrument, which was used in an earlier technical realization over sea ice [7], obtains observations at the five microwave frequencies 1.0 GHz, 2.3 GHz, 5.3 GHz, 10.0 GHz, and 15.0 GHz, (corresponding to L, S, C, X, and Ku band, respectively) and at all polarization combinations (HH, HV, VV, and VH). Each single measurement lasted one minute, followed by the compression and storage of the data (taking a few minutes).

3. RESULTS

Shown in Figure 1 are typical examples of non-calibrated radar Doppler spectra resulting from C-band measurements at an incident angle of 55° on December 18, 2011. The left panels are time-averaged Doppler spectra (averaged over one minute) for all polarization combinations (HH, HV, VV, VH; from top to bottom), the right panels are the respective time-resolving spectrograms of the same measurement.

The impact of enhanced surface roughness, including breaking gravity waves, is manifesting in a second maximum in the radar Doppler spectra at frequencies above 100 Hz. We note that this second maximum varies strongly between polarization combinations, resulting in an enhanced Doppler shift, f_{Dopp}, and Doppler bandwidth, BW, specifically for horizontal (HH), but also for cross (HV and VH) polarizations. Gray bars indicate the spectral range for which compute the radar backscatter and the spectral moments (see below). For the measurements shown the Doppler shifts at HH, HV, VV, and VH polarizations are 49.5 Hz, 35.1 Hz, 23.0 Hz, and 35.9 Hz, respectively.

In the right column of the figure respective time-resolved spectral modulations of the measured radar return (spectrograms) are displayed. Clearly visible is the temporal modulation of the measured Doppler spectra with peak amplitudes appearing at 10 sec and 37 sec of the displayed period. Inferred from the results can be a long surface gravity wave period of approximately 5 seconds, corresponding to a wavelength of approximately 40 m. The enhanced radar return amplitudes (spikes) in the

K.-W. Gurgel and T. Schlick were essential for making the instrument work. M. Fischer and F. Grawe assisted during the measurement campaign. The work presented herein was funded through an instrument-development grant from the University Hamburg, by the German Ministry of Education and Research (BMBF) under contract 03F0611E (SOPRAN) and by the CLISAP Excellence initiative, funded through a grant from the German Research Foundation (DFG) to the University of Hamburg.

spectrograms potentially can be attributed to the breaking of long surface gravity waves. We will focus in the following on the identification of those events through the change in the shape of the radar Doppler spectra.

The figure suggests that the Doppler spectra are intermittently broadened and then display secondary maxima, which possibly are linked to the occurrence of long surface gravity wave breaking. The observed alterations of the spectral shape manifests itself in changes in the second and fourth moments about the mean calculated as

$$M_2 = {}^1\!/\!_\sigma \cdot \sum[(f - f_{Dopp})^2\, \Psi(f)] \quad (1)$$

$$M_4 = {}^1\!/\!_\sigma \cdot \sum[(f - f_{Dopp})^4\, \Psi(f)] \quad (2)$$

with $f_{Dopp} = {}^1\!/\!_\sigma \cdot \sum[f\, \Psi(f)]$, $\sigma = \sum \Psi(f)$, and with $\Psi(f)$ being the measured power spectral density (PSD). The spectral bandwidth is $BW = 2 \cdot \sqrt{M_2}$, and summation (Σ) was performed over the grey-shaded frequency range (left panels in Figure 1), which corresponds to spectral power densities exceeding the -6dB limits of the spectral maximum. In the following we concentrate on modulations of those moments and their potential relation to breaking long surface gravity waves.

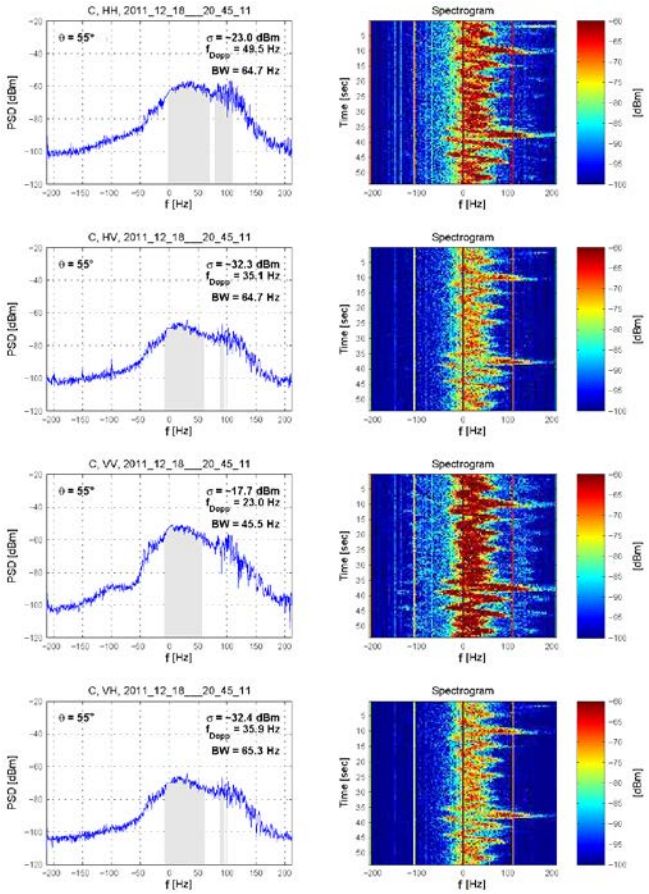

Figure 1. Example of non-calibrated C-band Doppler spectra (left column) and time-resolved spectrograms (right column) recorded on December 18, 2011 (incidence angle: 55°, wind: 12.5 m/s / 290°). Shown are all polarization combinations: HH, HV, VV, VH (top to bottom). Spectral parameters (radar cross section, σ, Doppler shift, f_{Dopp}, and Doppler bandwidth, *BW*, calculated from the gray-shaded spectral range) are inserted.

The standardized fourth moment, i.e. the ratio of the fourth over the squared second moments, $\beta = M_4/{M_2}^2$, can be used as a descriptor of the shape of a spectrum: lower values of β correspond to a greater bimodality [2], which in turn can be seen as an indicator for "heavy tails" in the corresponding spectrum. Consequently, high values of the reciprocal standardized fourth moment, $1/\beta$, might be used as an indicator for long-wave breaking. For a better comparison between the different radar bands, and to pronounce the effect of the widening of the spectral peak, we normalized it by the squared ratio of the half bandwidth and the radar frequency, f_R. The resulting normalized moment ratio, *NMR*, then reads:

$$NMR = {}^1\!/\!_\beta \cdot \left({}^{BW}\!/\!_{2} \over f_R\right)^2 = \frac{{M_2}^3}{M_4} \cdot \frac{1}{{f_R}^2} \quad (3)$$

Figure 2 shows those ratios for four radar bands (L, S, C, X; from top left to bottom right) and for the entire October 2012. Data, obtained at an incidence angle of 35° are colored in red, those of 45° incidence angle in green, and those of 55° incidence angle in blue. Only backscatter measurements were considered for conditions with wind blowing towards the westward looking antenna.

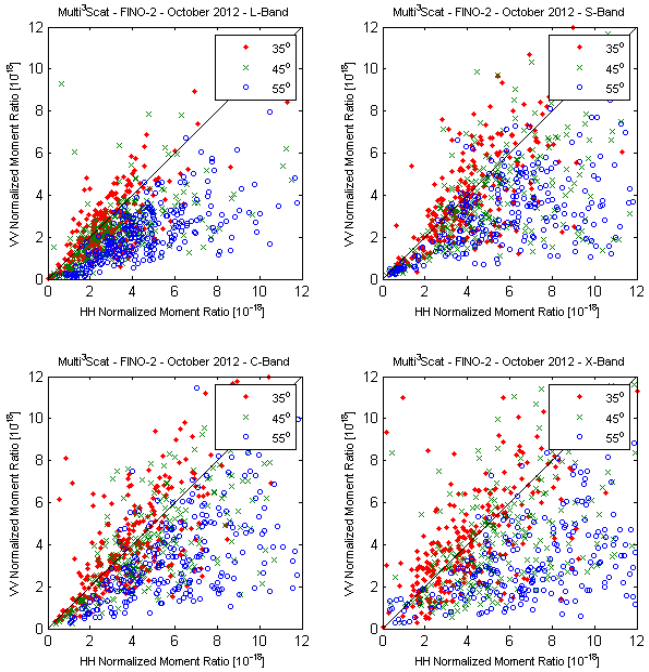

Figure 2. Normalized moment ratios, *NMR*, at HH (abscissa) and VV (ordinate) polarizations, for L, S, C, and X band (top left to bottom right). All upwind measurements in October 2012 were considered.

At 35° incidence angle (red dots) the normalized moment ratios, *NMR*, for HH and VV polarizations are comparable in size, but with increasing incidence angle (green crosses: 45°; blue circles: 55°) the normalized moment ratios for horizontal (HH) polarization grow faster than those for vertical (VV) polarization. This confirms that long-wave breaking has a stronger impact on the HH signal than on the VV signal, which is in accordance with earlier findings [1][5]. This effect seems present at all four radar bands; however, we also note that the scatter at higher *NMR* values becomes larger with increasing incidence angle and with increasing frequencies.

Before available visual and IR observations are evaluated with respect to breaking waves, we used, for simplicity, the so-called fractional area of whitecaps [8] as an indicator for the overall density of (spilling) wave breakers. The fractional area of whitecaps, *W*, is defined as [8]:

$$W = 1.95 \times 10^{-5} \cdot U^{2.55} \cdot \exp(0.0861\,\Delta T) \qquad (4)$$

where U is the wind speed at 10 m height and $\Delta T = T_w - T_a$ is the difference of the water temperature and air temperature and, thus, an approximation of atmospheric stability. Figure 3 demonstrates the dependence of the normalized moment ratios at S band on that fractional area of whitecaps. Dots correspond to an incidence angle of 35°, crosses to 45°, and circles to 55°.

Higher normalized moment ratios coincide with higher fractional areas of whitecaps. The data show a strong scatter at fractional whitecap areas exceeding 0.2% and at normalized moment ratios exceeding 2 [$\times 10^{-18}$]. In contrast, below both thresholds the scatter appears smaller. This threshold behavior might indicate that a certain density of long-wave breaking events is needed for a significant change in the shape of the radar Doppler spectra and,

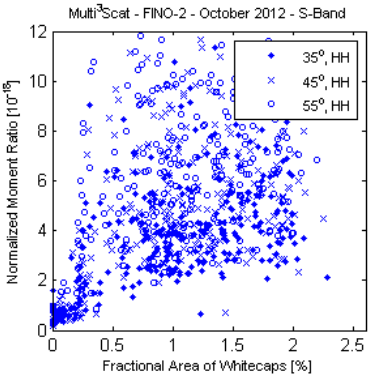

Figure 3. Normalized moment ratios as functions of the fractional area of whitecaps, for S-band HH-polarization. Each data point corresponds to a 1-minute measurement. Dots, crosses and circles denote incidence angles of 35°, 45° and 55°, respectively.

therefore, for a strong increase in the normalized moment ratios. It further suggests that it is suitable to define a threshold normalized moment ratio, which can be used to separate times of low and high fractional whitecap areas.

To test this hypothesis, we chose here 2 [$\times 10^{-18}$] as such a threshold value and selected those measurements, whose normalized moment ratios exceed this value. Figure 4 shows in green time series of the fractional whitecap area for the entire October 2012, based on wind and temperature measurements on FINO-2. Superimposed as red circles are those values, which correspond to times when radar measurements were carried out under upwind conditions. Then, based on the measurements at 55° incidence angle, blue asterisks mark those events that correspond to high (i.e., exceeding 2 [$\times 10^{-18}$]) normalized moment ratios calculated from S-band / HH-polarization data.

The measurements performed at times of small fractional whitecap areas (mainly corresponding to times of low wind speeds) also yielded small normalized moment

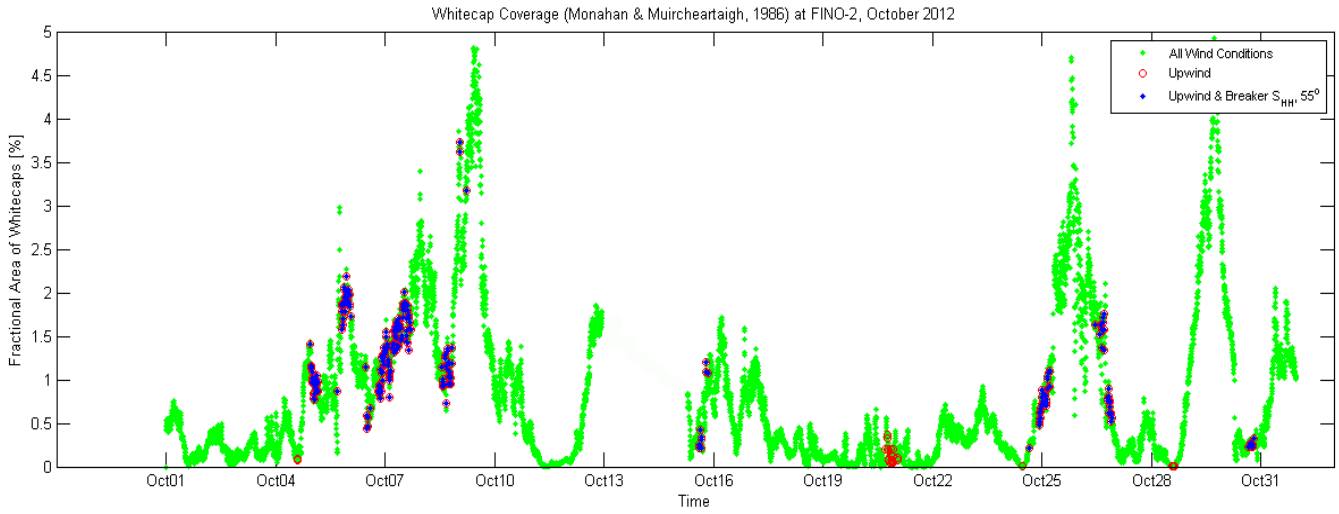

Figure 4. Time series of the fractional area of whitecaps for October 2012. Marked with red circles are upwind conditions, blue asterisks denote times of high normalized moment ratios derived from S-band (HH-polarization) data and from measurements at 55° incidence angle. The gap on October 13 and 14 was caused by extensive maintenance work on the platform.

ratios, and vice versa. During October 2012, wind speeds were roughly, between 5 m/s and 20 m/s, with only a few exceptions, when the wind speed was well below 5 m/s. At two of those dates, on late October 20 and on October 28, low westerly winds were recorded at FINO-2 and correspondingly, the normalized moment ratios derived from S-band HH data are below the given threshold, manifesting in red circles (without blue asterisks) at the respective dates in Figure 4.

Measurements at different incidence angles (not shown herein) yield almost the same results. This is in accordance with Figure 3, where no clear separation between the blue dots, crosses, and circles can be seen. We found similar results when we used HH-polarization data measured at other radar bands (L, C, and X; not shown herein). However, different results were obtained when VV-polarization data were used with the same threshold value (not shown herein), which can be explained by the different effect long-wave breaking has on the radar backscattering at HH and VV polarization (Figure 1).

4. CONCLUSIONS

A ratio of two spectral moments was used to relate radar backscatter measurements to the fractional area of whitecaps. In general, high normalized moment ratios occur at instances of large fractional whitecap areas, suggesting this ratio might be used as indicator for wave breaking. Our analyses indicate that S-band measurements at horizontal (HH) polarization are best suited to serve as input for such an indicator. Other radar bands seem less suitable. We note, however, that this analysis is very preliminary. To what extend results can be used as a universal algorithm and to what extend results can be improved through a combination of radar frequencies has yet to be investigated. Additional statistical indicators for the identification of wave-breaking events, as suggested in [3], might be required to generate wave-breaking statistics from surface backscatter signals.

REFERENCES

[1] Branch, R., W.J. Plant, M. Gade, and A.T. Jessup, "Relating Microwave Modulation to Microbreaking Observed in Infrared Imagery," *IEEE Geosci. Remote Sens. Lett., 5(3)*, 364-367, 2008.

[2] Darlington, R.B., "Is Kurtosis Really "Peakedness?", *American Statistician, 24(2)*, 19-22, 1970.

[3] Grobelny, A., 2013: "Analysis of breaking waves with scatterometer, optical and infrared data recorded at the FINO-2 platform," M.Sc. Thesis, University of Hamburg.

[4] Hara, T., and W.J. Plant, "Hydrodynamic modulation of short wind-wave spectra by long waves and its measurement using microwave backscatter," *J. Geophys. Res., 99(C5)*, 9767-9784, 1994.

[5] Jessup, A.T., W. Melville, and W. Keller, "Breaking waves affecting microwave backscatter 1. Detection and verification," *J. Geophys. Res., 96(C11)*, 20547-20559, 1991.

[6] Keller, W.C., and W.J. Plant, "Cross sections and modulation transfer functions at L and Ku bands measured during the tower ocean wave and radar dependence experiment," *J. Geophys. Res., 95(C9)*, 16277-16289, 1990.

[7] Kern, S., M. Brath, R. Fontes, M. Gade, K.-W. Gurgel, L. Kaleschke, G. Spreen, S. Schulz, A. Winderlich, and D. Stammer, "Multi³Scat -- A Helicopter-Based Scatterometer for Snow-Cover and Sea-Ice Investigations," *IEEE Geosci. Remote Sens. Lett., 6(4)*, 703-707, 2009.

[8] Monahan, E.C., and I.G. O'Muircheartaigh, "Whitecaps and the passive remote sensing of the ocean surface," *Int. J. Remote Sens., 7(5)*, 627-642, 1986.

[9] Plant, W.J., "A model for microwave Doppler sea return at high incidence angles: Bragg scattering from bound, tilted waves," *J. Geophys. Res., 102(C9)*, 21131-21146, 1997.

[10] Stammer, D., M. Gade, K.-W. Gurgel, and T. Schlick, "Multi-Frequency / Multi-Polarization Scatterometer Measurements in the Western Baltic Sea in support of air-sea flux studies", in preparation, 2014.